

Difficult control is related to instability in biologically inspired Boolean networks

Bryan C. Daniels^{1*} and Enrico Borriello^{1**}

¹School of Complex Adaptive Systems, Arizona State University, Tempe, AZ, USA

* bryan.daniels.1@asu.edu
** enrico.borriello@asu.edu

March 1, 2024

Abstract Previous work in Boolean dynamical networks has suggested that the number of components that must be controlled to select an existing attractor is typically set by the number of attractors admitted by the dynamics, with no dependence on the size of the network. Here we study the rare cases of networks that defy this expectation, with attractors that require controlling most nodes. We find empirically that unstable fixed points are the primary recurring characteristic of networks that prove more difficult to control. We describe an efficient way to identify unstable fixed points and show that, in both existing biological models and ensembles of random dynamics, we can better explain the variance of control kernel sizes by incorporating the prevalence of unstable fixed points. In the end, the fact that these exceptions are associated with dynamics that are unstable to small perturbations hints that they are likely an artifact of using deterministic models. These exceptions are likely to be biologically irrelevant, supporting the generality of easy controllability in biological networks.

1 Introduction

Since Kauffman’s original proposal [1] that the attractors of network dynamics could effectively represent different cell types, Boolean networks have found broad application in theoretical biology as the most parsimonious mathematical representation of real biological networks [2, 3].

In Ref. [4], we demonstrated that dynamic Boolean networks are often easy to control. We illustrated this on a large database of experimentally derived biological networks, as well as ensembles of random networks produced through several generating mechanisms. While various approaches have been proposed for quantifying the controllability of complex networks [5, 6, 7, 8, 9], we focus on the difficulty of steering the dynamics towards the

attractors of the unconstrained system [6], rather than navigating through all possible states [10]. This matches with the assumption that biological function is mostly captured by attractors, in that they represent the phenotypically and functionally distinct cell types expressed by the regulatory network [1].

Our findings reveal that, contrary to intuition, control toward existing attractors does not inherently become more difficult as the size of the network increases. Instead, a significantly more crucial factor is the number of attractor states generated by the dynamics. We find that the control needed to select one of the attractors typically grows logarithmically with the number of attractors. This concept is made precise by defining a *control kernel*: a set of nodes of minimal size whose states can be pinned to fixed values to force the system into a given attractor, regardless of initial conditions [11]. Our result can then be summarized in the statement that the average size of the control kernel of a dynamical Boolean network, $\langle |\text{CK}| \rangle$, typically scales logarithmically with the number of its attractors, r :

$$\langle |\text{CK}| \rangle \simeq \log_2 r. \quad (1)$$

In Ref. [4], we reinterpreted this result in terms of the conjectured expectation value of the witness set in computational learning theory [12]. More importantly, we view it as the most significant theoretical justification to date for the feasibility of genetic reprogramming [13].

While networks that were much more difficult to control than predicted by our scaling law were limited in number (roughly 2% of tested networks), we noted their occurrence in Ref. [4]. Specifically, some networks had significant numbers of attractors whose control required pinning nearly all nodes in the network. The presence of such networks, along with the unaccounted reasons for their difference from more easily controllable networks, could undermine one’s confidence in predicting the required level of control based solely on knowledge of a network’s attractors, as well as the hypothesis that a network’s size is typically irrelevant to the difficulty of control.

In this work, we investigate the factors that contribute to the increased difficulty in controlling exceptional networks. Our goal is to find approximations to the mean control kernel size that are simple to compute and do not rely on solving the full dynamics, which becomes intractable in moderately sized networks.

As a first step, we expand our database of biological networks by incorporating additional networks collected in Ref. [14], representing the most extensive collection of Boolean models for biological networks at the time of writing this manuscript. None of the new networks exhibit a significant deviation from our original predictions, leaving us with the task of explaining only the exceptions previously identified.

A direct examination of these exceptions highlights the role played in the controllability of the network by the presence of isolated fixed points, i.e., fixed points of the dynamics that do not attract any other state. We establish a strong correlation between this characteristic

and the difficulty of control, and we use this as the rationale for a correction to our original scaling law (Equation 1). The revised scaling law relies not only on the knowledge of the number of attractors but also on the number of isolated fixed points among them. Interestingly, the latter can be easily evaluated even for networks where not all basin sizes are known, particularly in cases where the identity of all attractors can be obtained by exploiting modularity in the network topology. We test whether our new empirical formula outperforms our previous scaling law, and demonstrate that it accounts for the majority of the remaining variance not captured by the original scaling.

In the next section (*Results*), we describe our extended analysis and provide the correction to our empirical formula.

In the *Methods* section, we show how we leverage the modular structure of biological networks to identify the complete spectrum of their attractor states, and we demonstrate how to exploit the sparse connectivity of these networks to identify all isolated fixed-points by explicitly determining their backward reachable sets, i.e., the sets of their pre-images.

Finally, in the *Discussion* section, we comment on the biological relevance of these isolated fixed-points.

2 Results

To explore the drivers of exceptionally large control kernels, we first ask: What is the maximum possible control kernel size for a given network? Given our definition of control, fixed-point attractors always have a control kernel, as control can be attained by pinning all nodes in the network. Note that cyclic attractors are sometimes not able to be forced with static control because we are limited to pinning non-cycling nodes — in these cases, we say that a control kernel does not exist. This sets the simplest upper bound on the size of control kernels for controllable attractors of $|\text{CK}| \leq n$. A more economical approach avoids pinning nodes in any peripheral trees that are wholly dependent on nodes within closed feedback loops in the regulatory network topology. We will refer to the network’s core as the set of nodes that exclude any peripheral trees, with a number of core nodes n_c . As control kernels are defined as sets of controlling nodes of minimal size, we can ensure a tighter bound of $|\text{CK}| \leq n_c$.

We might naively expect that it would be more difficult to steer the system toward attractors that are less likely to be found when initializing the system in a random state. Therefore, one might expect extreme control kernel sizes for attractors with very small basins of attraction (defined as the states that lead to each attractor under the dynamics). While basin sizes are not generally easy to compute, it is relatively simple to highlight the most extreme scenarios when an attractor is an “isolated” fixed point, i.e., with a basin size of 1 (see Methods).

Both isolated fixed points and maximal control kernel sizes ($|\text{CK}| = n_c$) are connected to concepts of instability (Fig. 1). First, fixed points with maximal control kernels are

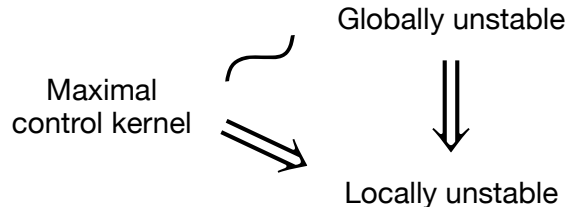


Figure 1: **Summary of the logical relationships between the stability of a fixed point and whether it has a control kernel of maximal size.** A fixed point with maximal control kernel size ($|\text{CK}| = n_c$) is always locally unstable, as is one that is globally unstable. Global instability is correlated with maximal control kernel size in the ensembles we study, but neither implies the other in general. Here local instability means that all states at Hamming distance 1 are in the basins of other attractors, and global instability means that no other states lead to the fixed point (basin size = 1).

locally unstable, in the sense that such a fixed point must be unstable to individual bit flips. That is, each state at Hamming distance 1 from the fixed point must be in the basin of a different attractor (otherwise one of the nodes could be left unpinned and the system would still return to the fixed point). Note that local instability does not necessarily imply that no other states transition into the fixed point under the dynamics. Also, while having a maximal control kernel implies local instability, local instability does not in itself guarantee a maximal control kernel. Second, isolated fixed points are globally unstable, in the sense that no other states transition into them.¹ Though a fixed point being globally unstable does not directly imply that it has a maximal control kernel, we might expect some correlation between instability and difficulty of control.

In Fig. 2, we compare average control kernel sizes in networks that have isolated (globally unstable) fixed points to the distribution over all networks (A and B) and control kernel sizes for individual isolated fixed points compared to the distribution over all attractors (C and D). The control kernel sizes of isolated fixed points are often close to n_c , matching with our intuition. Some of the biological networks have no feedback loops and are therefore controlled entirely by their input nodes, which trivially creates isolated fixed points with $|\text{CK}| = n_c$ (hatched areas in Fig. 2). Even aside from this effect, isolated fixed points tend to have very large control kernels.

Thus, though global instability does not always imply difficult control, the correlation is nonetheless striking in the ensembles that we study. In fact, we find in our network ensembles that fixed points with maximal control kernels occur only in networks that have at least one globally unstable fixed point (Table 1).

At the level of individual networks and attractors there are exceptions to the rule that

¹This is distinct from other notions of instability in the literature on Boolean networks, such as instability of cycles to delays in updating [15].

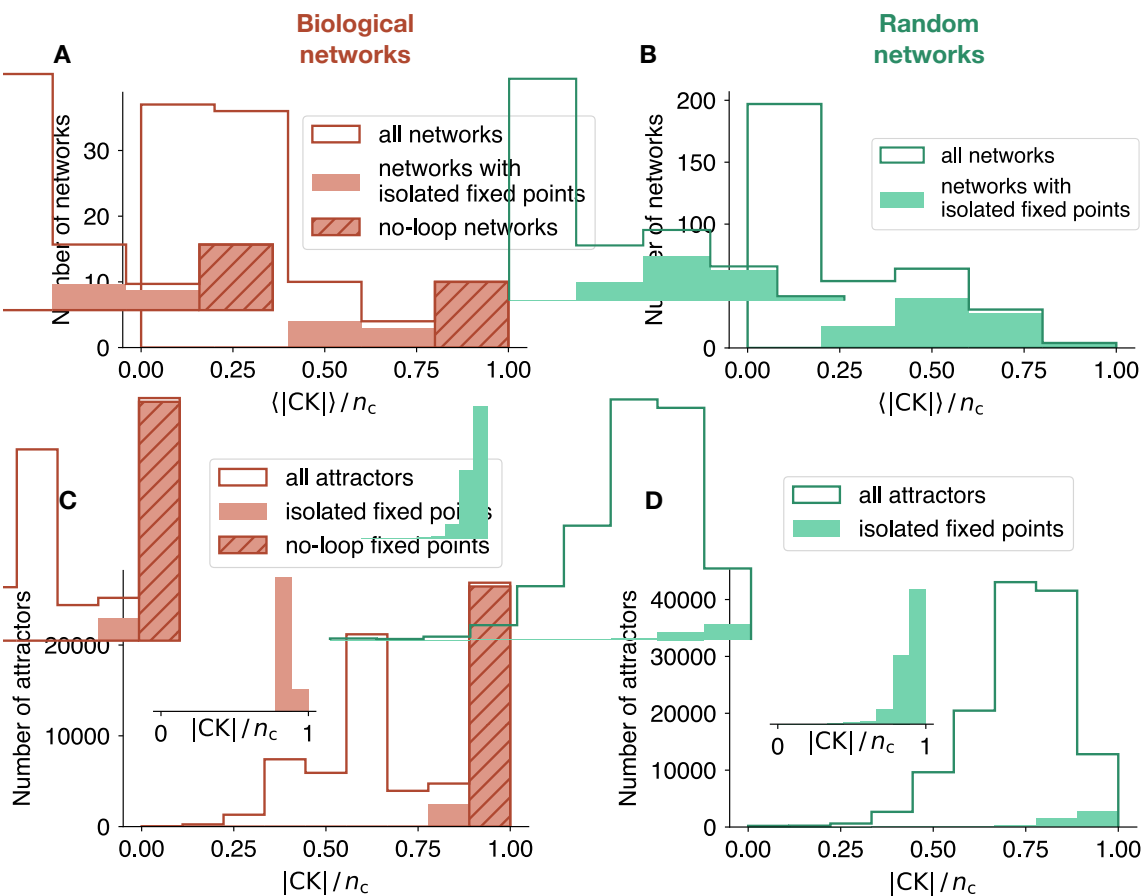


Figure 2: **Isolated fixed points are related to large control kernel sizes.** Both when averaged across attractors within networks (A and B) and at the level of individual attractors (C and D), isolated fixed points (those with basin size = 1; shaded bars) produce control kernel sizes $|CK|$ that are large relative to the total number of core nodes n_c . This pattern holds in both the biological (A and C) and random (B and D) network ensembles that we study. Some of the biological networks have no feedback loops, which trivially creates isolated fixed points with $|CK| = n_c$ (hatched bars in A and C). Insets in C and D highlight the distributions of control kernel sizes for only the isolated fixed points in networks that do contain feedback loops.

	Total	Controllable	With Isolated	With Max CK	With Both
Biological networks	104	97	17	16	16
Random networks	371	346	87	73	73

Table 1: **Summary of the analyzed networks.** “Total” includes all networks for which we can compute attractors and control kernels exactly. “Controllable” includes all networks for which static control kernels exist for a non-negligible set of attractors (here set as a threshold that the basins of uncontrollable cycles must make up less than 99% of the state space). “With Isolated” includes networks that have at least one isolated fixed point. “With Max CK” includes networks that have at least one fixed point with $|\text{CK}| = n_c$. “With Both” includes networks that have nonzero numbers of both isolated fixed points and maximal control kernels. (Note: 10 of the biological networks have no loops, which implies that all of their attractors are isolated and control kernels are of maximal size.)

globally unstable fixed points tend to be difficult to control. See SI Fig. S1 and Fig. S2 for histograms of control kernel sizes within each network that has at least one globally unstable fixed point. (In one network from the random ensemble, a globally unstable fixed point in fact has the smallest control kernel of all the network’s attractors.) Yet these exceptions are rare.

Given that it is relatively fast to determine whether a given fixed point is globally unstable (see Methods), and these are also the ones that tend to contribute most to changes in $\langle |\text{CK}| \rangle$, we propose using their number to get a computationally simpler estimate of control kernel sizes. If we assume that isolated fixed points are the only ones contributing to the difference from Eq. 1 and that they have the maximum possible size n_c , we get the approximation

$$\langle |\text{CK}| \rangle \simeq \frac{r-s}{r} \log_2 r + \frac{s}{r} n_c, \quad (2)$$

where s is the number of isolated fixed-points. As shown in Fig. 3, this simple estimate does quite well in most cases, outperforming Eq. 1 for almost all networks we tested.

The significance of Eq. 2 lies in the fact that, similar to Eq. 1, it enables an estimation of the average control kernel size solely based on the characteristics of the attractor landscape of the dynamics. This is achieved without the necessity of solving the NP-hard problem of determining control kernels for all r attractors.

Fig. 4 illustrates the initial variance in the distribution of $\langle |\text{CK}| \rangle$ across the analyzed biological and random networks. This variance can be better explained by our new predictor in Eq. 2 as compared to the previous predictor in Eq. 1. The improved precision in the new estimation is attained by integrating additional information, specifically the number s of isolated fixed points within the landscape, which is the primary cause for the deviations from our simple estimate.

Significantly, Eq. 2 introduces a dependence of the control kernel on the network size (specifically on n_c). This seems to be at odds with our findings in Ref. [4], where we

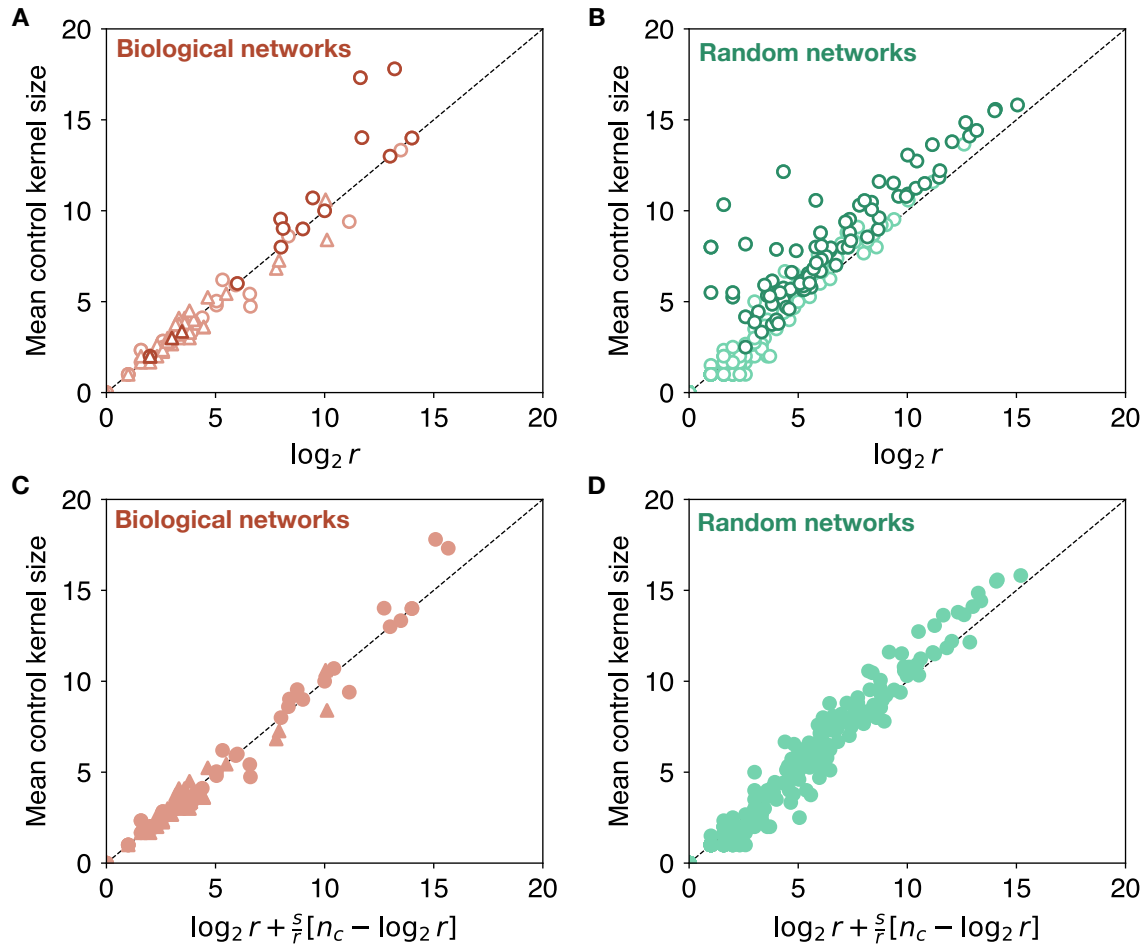


Figure 3: **A correction that incorporates the number of isolated fixed points leads to better predictions of control kernel sizes.** (A and B) The simple prediction that the mean control kernel size within each network is equal to the logarithm of the number of attractors r (Eq. 1) works well for most networks, but there are a number of exceptional networks that are much harder to control than expected. These exceptional networks all have isolated fixed points (highlighted with a darker color). (C and D) A correction that assumes isolated fixed points have control kernel of size n_c (Eq. 2) leads to better predictions.

concluded that the average control kernel size remains independent of the network size. It is crucial to note that the parameter s is typically small in comparison to r , so that the influence of n_c is often hidden upon considering an average across all attractors in a network. This becomes especially apparent when Eq. 2 is recast in the form

$$\langle |\text{CK}| \rangle \simeq \log_2 r + \frac{s}{r} \left[n_c - \log_2 r \right], \quad (3)$$

which shows how the size-dependent contribution is a correction to Eq. 1 whose relevance scales with the fraction s/r of isolated fixed-points.

Once analyzed in the context of their biological relevance, we may expect the dependence on n_c to be even less impactful in real-world dynamics. The presence of isolated fixed-point attractors, which arise in models with deterministic updating rules, is undermined by the incorporation of stochasticity in more realistic models of gene regulation (see *Discussion*).

3 Methods

Boolean network dynamics and control kernels. In a Boolean network, the states of individual components in a system are represented as Boolean variables that are updated in discrete timesteps according to fixed logical rules. Here we use a synchronous updating scheme, which creates deterministic dynamics. After transient dynamics, all initial states lead to a set of attractors that represent the possible long-term behaviors of the system. Each attractor consists either of a single state (fixed point) or cycles through a larger set of states.

We characterize the difficulty of control using the notion of a control kernel [11]. Specifically, we define a control kernel for a given attractor as a set of nodes of minimal size that can be statically pinned to fixed values such that, in the pinned dynamics, all initial conditions converge to the desired attractor. Using this static definition of control, all fixed point attractors have a control kernel of some size, but not all cycles are controllable.

For set environmental conditions (i.e. fixed states of input nodes [4]) multiple attractors can only exist if the network structure presents feedback loops [6]. Any set of nodes connected in a tree structure without closed loops will depend deterministically on the states of input nodes in each attractor state. For this reason, nodes outside of a feedback loop will never be part of a control kernel (as all behavior of trees will be fully controlled once the attractor is selected within the core). For this reason, we remove from our analysis all dependent trees of nodes from each network, leaving only a number $n_c \leq n$ of “core” nodes that participate in feedback loops and have the potential to be part of control kernels. Alternatively, we could include all n nodes in our analysis, but this would preclude the possibility of having any isolated fixed points in networks that have any nodes on which no other nodes depend (as changing the states of such nodes does not affect the dynamics).

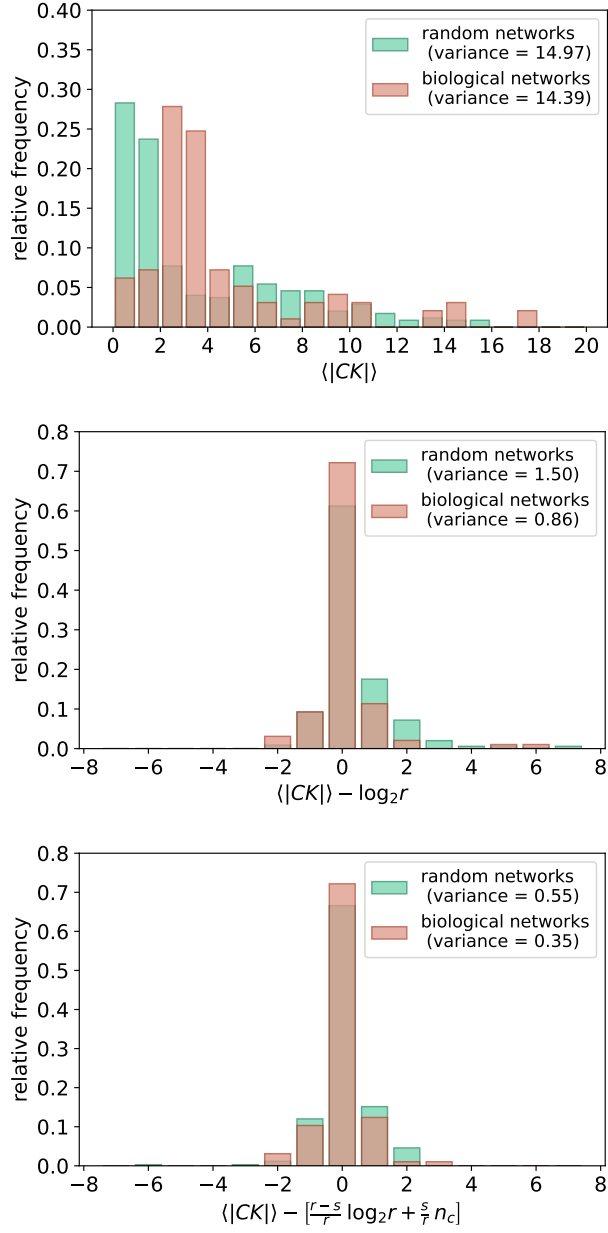


Figure 4: **The isolated fixed point correction reduces the variance of mean control kernel size predictions.** (A) The distributions of mean control kernel sizes across the ensembles of biological and random networks have large variances (listed in the legend). (B) Most of this variance can be explained in terms of the number of attractors r as in Eq. 1. (C) A large fraction of the remaining variance is explained by using the corrected Eq. 2 that incorporates the number of isolated fixed points s .

Network ensembles. For this study, we complement the set of network models analyzed in Ref. [4] with the more recent database compiled by Kadelka et al. [14] consisting of 122 Boolean models of biological regulation. The models in this database were chosen from a pool of 163 models identified using the Pubmed biomedical literature search engine, further restricted to include only expert-curated models (where both nodes and update rules were manually selected to prevent artifacts induced by prediction algorithms) and only one version of closely related models. Out of the 122 models, 61 were present in the Cell Collective database [16] that we analyzed in Ref. [4]. For consistency with our previous work, we retain a small number of Cell Collective networks that were not included in the Kadelka et al. database. The resulting set of networks encompasses models describing the regulatory logic governing various processes across a diverse array of species spanning different kingdoms of life, including animals, plants, fungi, and bacteria. For additional details, see Ref. [14] and its supplementary information.

To increase the variance in our tested models, we also include three ensembles of random Boolean networks, as presented in Ref. [4]. These include Kauffman networks with random truth tables, as well as Erdos–Renyi networks governed by threshold rules, with thresholds chosen either at zero total input or balanced to account for the number of inputs to each node (for details, see Ref. [4]).

We use a slightly stricter criterion for choosing networks to include here than in previous work [4]. As before, we only include networks for which attractors and control kernels can be computed with a reasonable amount of computer time (about 1 day of compute time on a single CPU), and we further restrict ourselves to include only networks for which we are able to compute attractors exactly, without relying on sampling. We are able to compute exact attractors and control kernels for 104 biological networks (out of 122) and 371 random networks (out of 375). Furthermore, a limited number of networks (7 out of 104 biological networks and 25 out of 371 random networks) are characterized by uncontrollable cycles with basins that cumulatively comprise more than 99% of the state space. Due to the static nature of the control kernel examined in this study, we filter out these networks from further analysis.

Complete lists of networks analyzed in this work are included as comma separated files in the supplementary material, and the biological networks are listed in Tables S1 and S2.

Modularity. Biological regulatory network models often exhibit high modularity in their topology, where subsets of nodes interact more intensely within their own subsets than with other subsets. Additionally, these models tend to be hierarchical, featuring upstream modules that operate independently of downstream module behavior [17].

Efficient computation of attractors in modular and hierarchical Boolean networks can be achieved by analyzing modules separately. The approach involves identifying attractors for upstream modules first and subsequently leveraging each upstream attractor to determine corresponding attractors for downstream modules. Despite some intricacies discussed below, the computational execution of this process remains straightforward.

We first decompose a given Boolean dynamical system into hierarchical modules, defined as strongly connected components within the system’s causal network. This representation is in the form of a directed acyclic graph, capturing dependencies among modules. We then identify attractors for upstream modules that are independent of others, utilizing a brute-force approach iterating over all possible states within the module.

For each downstream module \mathcal{D} , attractors \mathbf{U} of upstream modules, on which \mathcal{D} relies, are explored through all possible combinations. Given an attractor $U \in \mathbf{U}$, the states of nodes in upstream modules are fixed to the values present in U , and corresponding attractors for \mathcal{D} are determined using a brute-force approach iterating over all possible dynamics of \mathcal{D} based on the input from U .

Two subtleties arise when computing the set of all possible attractors \mathbf{U} for nodes upstream of \mathcal{D} . In the simplest case, where \mathcal{D} depends on separate modules $\mathcal{U}_1, \mathcal{U}_2, \dots, \mathcal{U}_n$ without shared ancestor modules, and all corresponding sets of upstream attractors $\mathbf{U}_1, \mathbf{U}_2, \dots, \mathbf{U}_n$ consist only of fixed points, \mathbf{U} comprises $\prod_i |\mathbf{U}_i|$ attractors. However, when upstream modules share ancestor modules further upstream, or when dealing with cyclic attractors of length $\ell > 1$, additional considerations are necessary to account for inconsistent combinations and phase shifts between attractors, respectively.

We use this modular approach to efficiently identify attractors and compute control kernels. For more details, see Ref. [4].

Backward Reachable Sets. Equation 2 relies on evaluating the basin sizes, a non-trivial task. To find basin sizes, one must solve for the equilibrium dynamics starting from every state of the system. The size of the network becomes a limiting factor due to the exponential growth of the number of states. While we can capture the entire set of attractor states for networks as large as ~ 300 nodes by leveraging the modular structure of their topology (see *Modularity* subsection above), this approach does not directly produce basin sizes. For smaller networks, we can directly compute them, but for the larger biological networks, this is infeasible. While we can sample a fixed number of initial conditions to estimate basin sizes, our inability to distinguish attractors that we never find in sampling from those with very small basin size limits the usefulness of this approach. Instead, we will leverage the knowledge of the attractors’ identities and the fact that in Eq. 2 we only need to know the number of them that are isolated.

In what follows, we present an efficient strategy for identifying the backwards reachable set of states in a Boolean network. We employ this method to quantify the exact number of isolated attractors s within the complete set of attractors r identified using the modular approach.

Let us refer to a generic Boolean network with n nodes and updating rules

$$\begin{aligned} x'_1 &= f_1(x_1, \dots, x_n) \\ \dots & \\ x'_n &= f_n(x_1, \dots, x_n), \end{aligned} \tag{4}$$

where x_i is the value (0 or 1) of node i at time t , and x'_i is its value at time $t+1$. We will call $S_{i,b}$ the subset of the configuration space S containing all the states satisfying the non-linear equation $f_i(x_1, \dots, x_n) = b$, where $b = 0, 1$. Therefore, given a state $X = (x_1, \dots, x_n)$, its backward reachable set, defined as the set of its pre-images, is

$$S_X = S_{1,x_1} \cap S_{2,x_2} \cap \dots \cap S_{n,x_n} . \quad (5)$$

Finding the $2n$ sets $S_{i,b}$ is equivalent to finding the pre-images of each state in S . A straightforward algorithm for finding $S_{i,b}$ would evaluate $f_i(x_1, \dots, x_n)$ for all $(x_1, \dots, x_n) \in S$, and select all the states for which $f_i(x_1, \dots, x_n) = b$. This approach would require $2n \times 2^n$ operations, as opposed to the $n \times 2^n$ operations we would need to determine the entire forward evolution of the network. In general, using a reverse algorithm is not a better way of solving the dynamics of a network [18]. Yet for our problem we only need to find the backward reachable sets for each known fixed point, to determine if its only pre-image is itself and it is therefore an isolated fixed point. From a computational standpoint, additional simplifications arise from the fact that the in-degree of the nodes in the network, i.e., the average number of inputs in the f_i functions, is often much smaller than n . Considering this, a more efficient method for performing the intersection in Eq. 5 is to employ a parametric approach based on conditions solely related to the variables involved in each Boolean function.

If we call $P_{i,b}$ the set of sets of parametric equations defining the elements of $S_{i,b}$, then the set of sets of equations defining the elements of S_X is

$$P_X = P_{1,x_1} \bar{\times} P_{2,x_2} \bar{\times} \dots \bar{\times} P_{n,x_n} ,$$

where $\bar{\times}$ denotes an *unordered* and *repetition-free* Cartesian product of sets, from which sets containing *inconsistent equations have been removed*.

Examples: Providing examples will help clarify our method. One benefit of referencing the parametric sets $P_{i,b}$ is that they serve as a highly concise representation of the sets $S_{i,b}$ when they encompass substantial subsets of the state space. For instance, an updating function with only k inputs will impose constraints solely on the k variables involved, leaving the remaining $n - k$ unconstrained. The number of combinations of these k variables will be multiplied by the 2^{n-k} number of combinations of the unconstrained variables. It is not uncommon in the biological networks we study to encounter functions with only one input out of tens of possible genes. In a scenario like this, having just twenty nodes can result in the order of the set $S_{i,b}$ being half a million, but its parametric set $P_{i,b}$ includes only one condition for its input.

Next, let us examine an example of how the products of the $P_{i,b}$ sets are calculated. For simplicity, we will refer to the smallest biological network in our database: a gene regulatory network model for mammalian cortical area development from Ref. [19]. This model comprises just five genes: *Coup_fti*, *Emx2*, *Fgf8*, *Sp8*, and *Pax6*. The network admits

two fixed-point attractors, $X_1 = [0, 0, 1, 1, 1]$ and $X_2 = [1, 1, 0, 0, 0]$ (neither of them being isolated). Let us find the pre-images of X_1 . From the updating rules

$$\begin{aligned}
Coup_fti &= \overline{Sp8 \text{ OR } Fgf8} \\
Emx2 &= Coup_fti \text{ AND } \overline{Fgf8} \text{ AND } \overline{Pax6} \text{ AND } \overline{Sp8} \\
Fgf8 &= Fgf8 \text{ AND } Sp8 \text{ AND } \overline{Emx2} \\
Sp8 &= Fgf8 \text{ AND } \overline{Emx2} \\
Pax6 &= Sp8 \text{ AND } \overline{Coup_fti} \text{ AND } \overline{Emx2}
\end{aligned}$$

(where an overline represents the Boolean operator **NOT**) we can deduce the parametric sets relevant to X_1 :

$$\begin{aligned}
P_{Coup_fti,0} &= \{\{Sp8 = 1\}, \\
&\quad \{Fgf8 = 1, Sp8 = 0\}\} \\
P_{Emx2,0} &= \{\{Coup_fti = 0\}, \\
&\quad \{Coup_fti = 1, Fgf8 = 1\}, \\
&\quad \{Coup_fti = 1, Fgf8 = 0, Pax6 = 1\}, \\
&\quad \{Coup_fti = 1, Fgf8 = 0, Sp8 = 1, Pax6 = 0\}\} \\
P_{Fgf8,1} &= \{\{Fgf8 = 1, Emx2 = 0, Sp8 = 1\}\} \\
P_{Sp8,1} &= \{\{Emx2 = 0, Fgf8 = 1\}\} \\
P_{Pax6,1} &= \{\{Coup_fti = 0, Emx2 = 0, Sp8 = 1\}\} .
\end{aligned}$$

For example,

$$P_{Coup_fti,0} \bar{\times} P_{Fgf8,1} = \{\{Fgf8 = 1, Emx2 = 0, Sp8 = 1\}\} = P_{Fgf8,1} ,$$

because the products including the contradicting conditions $Sp8 = 0$ and $Sp8 = 1$ have been removed.

Once all five sets are multiplied, the result is

$$P_{X_1} = \{\{Coup_fti = 0, Emx2 = 0, Fgf8 = 1, Sp8 = 1\}\} .$$

As no condition is set on $Pax6$,

$$S_{X_1} = \{[0, 0, 1, 1, 0], [0, 0, 1, 1, 1]\} .$$

One of the two pre-images is just X_1 , as expected from that fact that it is a fixed-point.

For isolated fixed-points, this calculation returns a set of order one, where the only element is the fixed-point itself. Therefore, for each network, we perform this test on all of its fixed-points in order to count the number s of them that are isolated.

In computational terms, each set $P_{i,b}$ is essentially a dataframe. This dataframe has columns representing the input nodes of the function f_i , and each row corresponds to a combination of dynamic variables (node dynamical states) for which f_i evaluates to b_i . The solution to the problem involves obtaining the result sequentially by taking Cartesian products of all n dataframes and subsequently eliminating inconsistent rows.

A potential complication arises from a temporary combinatorial growth in the number of rows when products are computed between conditions over functions that do not share many inputs. This occurs when there are few cancellations. To address this, we initially conduct a Louvain community detection analysis on the network [20]. We then perform the first round of products among dataframes associated with functions that exhibit the highest overlap among their inputs. Finally, we conduct the ultimate round of products among the results obtained in this manner. (This is computationally more efficient than using the modular structure for the first round of products, as it removes the limitation imposed by having a strict hierarchical structure.) This approach provides an efficient method for determining the backward reachable sets of our candidate isolated points.

4 Discussion

A comprehensive understanding of biological control is fundamental for both practical applications, such as genetic reprogramming [13, 21], regenerative medicine [22], and drug design [23, 24, 25], and for advancing our theoretical understanding of cellular coordination in systems biology [26]. As we explore the intricacies of controlling biological systems, essential questions arise: How easily can we exert control over these systems? What factors in a system’s design and behavior contribute to the ease or difficulty of control?

With a few notable exceptions, our previous work indicated that the average required level of control primarily depends on the number of preexisting attractors and shows no dependence on the system’s size. While these exceptions were not numerous enough to undermine the general trend of ‘easy controllability’, they raised the question of whether biological systems exist that are inherently harder to control.

This work represents a more in-depth analysis of these exceptions. Similarly to Ref. [4], we compare the results from our database of biological networks to those obtained in several ensembles of systems with randomly assigned network topologies and dynamic rules. These random ensembles are particularly important to include in that they produce a larger number of harder to control networks. Additionally, we roughly doubled the number of biological networks we tested (increasing from 49 to 104 models) through the inclusion of networks cataloged in Ref. [14]. Importantly, no new exceptions to our original scaling law were observed.

Our primary observation here unveils a consistent pattern in these exceptions, found in both the biological and random ensembles. This pattern originates from the presence of isolated fixed points—fixed points that attract no other states and prove to be among

the attractors most challenging to control, with a control kernel that often includes all or almost all core nodes in the network.

Why is there a connection between unstable fixed points and difficult control? One simple way to get both instability and difficult control is exemplified in our random network ensemble that uses threshold updating rules. When thresholds are set uniformly low, this leads to a bias toward activation: the dynamics tend to push toward states with more 1s than 0s. States with few or no 1s can sometimes map to themselves, forming isolated fixed points. These states are also difficult to control because any node that is allowed to be active leads away toward further spreading of activation.

Unfortunately, this connection between unstable fixed points and difficult control itself has exceptions. In particular, it is possible to construct networks that are difficult to control without having globally unstable fixed points.² Still, by efficiently counting the unstable fixed points of a network, we are able to better explain the variance in control kernel sizes by incorporating the prevalence of these unstable fixed points. This constitutes a useful tool to predict the expected amount of required control over a network based solely on partial information of the attractor landscape, thus avoiding the NP-hard problem of evaluating individual control kernels.

The observation that difficult control is related to unstable fixed points is reassuring for several reasons. Firstly, these fixed points likely result from the strict deterministic nature of updates in the considered biological models. Most sources of stochasticity [27] would likely push the dynamics onto a path leading to a more stable attractor characterized by an adjacent basin of non-negligible size. More importantly, this same property makes it highly improbable for such states to carry biological significance, i.e., to represent actual cell types. Their persistence would require fine-tuned preservation of an unstable dynamical state.

The biological irrelevance of such unstable fixed points is also significant for another reason. As they reintroduce an explicit dependence on the network size, these exceptions would contradict our main statement that control does not scale with the size of the system [4], in direct disagreement with recent results in the genetic reprogramming of mammalian cells [13]. In this light, we interpret our correction (Equation 2) as an empirical method for obtaining a more precise estimate of the required control when employing a simplistic, deterministic model of the regulatory dynamics. Verifying that our size-independent scaling law remains valid in models of genetic regulation that include stochasticity is needed but beyond the scope of this work.

More generally, given our results one might hope that the amount of control necessary to select macroscopic phenotypes could be approximated without knowing details of the microscopic dynamics.

²We describe one such exception in the SI, a network dynamic in which a locally unstable fixed point has maximally distant network states that map back to it. We find only one similar network in the random ensembles that we study, and we conjecture that such contrived examples are unlikely in real biological systems.

References

- [1] Stuart A Kauffman. Metabolic stability and epigenesis in randomly constructed genetic nets. *Journal of theoretical biology*, 22(3):437–467, 1969.
- [2] F Vladimir. Handbook of computational molecular biology. *University of California, Davis*, 2005.
- [3] Adrien Fauré, Aurélien Naldi, Claudine Chaouiya, and Denis Thieffry. Dynamical analysis of a generic boolean model for the control of the mammalian cell cycle. *Bioinformatics*, 22(14):e124–e131, 2006.
- [4] Enrico Borriello and Bryan C Daniels. The basis of easy controllability in boolean networks. *Nature communications*, 12(1):5227, 2021.
- [5] Jorge GT Zanudo and Réka Albert. Cell fate reprogramming by control of intracellular network dynamics. *PLoS computational biology*, 11(4):e1004193, 2015.
- [6] Jorge Gomez Tejeda Zañudo, Gang Yang, and Réka Albert. Structure-based control of complex networks with nonlinear dynamics. *Proceedings of the National Academy of Sciences*, 114(28):7234–7239, 2017.
- [7] Bernold Fiedler, Atsushi Mochizuki, Gen Kurosawa, and Daisuke Saito. Dynamics and control at feedback vertex sets. i: Informative and determining nodes in regulatory networks. *Journal of Dynamics and Differential Equations*, 25:563–604, 2013.
- [8] Atsushi Mochizuki, Bernold Fiedler, Gen Kurosawa, and Daisuke Saito. Dynamics and control at feedback vertex sets. ii: A faithful monitor to determine the diversity of molecular activities in regulatory networks. *Journal of theoretical biology*, 335:130–146, 2013.
- [9] Isaac Crespo, Thanneer M Perumal, Wiktor Jurkowski, and Antonio Del Sol. Detecting cellular reprogramming determinants by differential stability analysis of gene regulatory networks. *BMC systems biology*, 7(1):1–14, 2013.
- [10] Yang-Yu Liu, Jean-Jacques Slotine, and Albert-László Barabási. Controllability of complex networks. *nature*, 473(7346):167–173, 2011.
- [11] Junil Kim, Sang-Min Park, and Kwang-Hyun Cho. Discovery of a kernel for controlling biomolecular regulatory networks. *Scientific reports*, 3:2223, 2013.
- [12] Eyal Kushilevitz, Nathan Linial, Yuri Rabinovich, and Michael Saks. Witness sets for families of binary vectors. *Journal of Combinatorial Theory, Series A*, 73(2):376–380, 1996.

- [13] Franz Josef Müller and Andreas Schuppert. Few inputs can reprogram biological networks. *Nature*, 478(7369):2–3, 2011.
- [14] Claus Kadelka, Taras-Michael Butrie, Evan Hilton, Jack Kinseth, Addison Schmidt, and Haris Serdarevic. A meta-analysis of boolean network models reveals design principles of gene regulatory networks. *arXiv preprint arXiv:2009.01216*, 2020.
- [15] Konstantin Klemm and Stefan Bornholdt. Stable and unstable attractors in Boolean networks. *Physical Review E - Statistical, Nonlinear, and Soft Matter Physics*, 72(5):1–4, 2005.
- [16] Tomáš Helikar, Bryan Kowal, Sean McClenathan, Mitchell Bruckner, Thaine Rowley, Alex Madrahimov, Ben Wicks, Manish Shrestha, Kahani Limbu, and Jim A Rogers. The Cell Collective: toward an open and collaborative approach to systems biology. *BMC systems biology*, 6:96, 2012.
- [17] Soumya Paul, Cui Su, Jun Pang, and Andrzej Mizera. A decomposition-based approach towards the control of boolean networks. In *Proceedings of the 2018 ACM International Conference on Bioinformatics, Computational Biology, and Health Informatics*, pages 11–20, 2018.
- [18] Andrew Wuensche, Mike Lesser, and Michael J Lesser. *Global dynamics of cellular automata: an atlas of basin of attraction fields of one-dimensional cellular automata*, volume 1. Andrew Wuensche, 1992.
- [19] Clare E Giacomantonio and Geoffrey J Goodhill. A boolean model of the gene regulatory network underlying mammalian cortical area development. *PLoS computational biology*, 6(9):e1000936, 2010.
- [20] Vincent D Blondel, Jean-Loup Guillaume, Renaud Lambiotte, and Etienne Lefebvre. Fast unfolding of communities in large networks. *Journal of statistical mechanics: theory and experiment*, 2008(10):P10008, 2008.
- [21] Kenji Kamimoto, Mohd Tayyab Adil, Kunal Jindal, Christy M Hoffmann, Wenjun Kong, Xue Yang, and Samantha A Morris. Gene regulatory network reconfiguration in direct lineage reprogramming. *Stem Cell Reports*, 18(1):97–112, 2023.
- [22] Mukul Tewary, Nika Shakiba, and Peter W Zandstra. Stem cell bioengineering: building from stem cell biology. *Nature Reviews Genetics*, 19(10):595–614, 2018.
- [23] Sourish Ghosh and Anirban Basu. Network medicine in drug design: implications for neuroinflammation. *Drug discovery today*, 17(11-12):600–607, 2012.
- [24] Kristen Fortney, Wing Xie, Max Kotlyar, Joshua Griesman, Yulia Kotseruba, and Igor Jurisica. Networkx: connecting drugs to networks and phenotypes in *saccharomyces cerevisiae*. *Nucleic acids research*, 41(D1):D720–D727, 2012.

- [25] Justin Lamb, Emily D Crawford, David Peck, Joshua W Modell, Irene C Blat, Matthew J Wrobel, Jim Lerner, Jean-Philippe Brunet, Aravind Subramanian, Kenneth N Ross, et al. The connectivity map: using gene-expression signatures to connect small molecules, genes, and disease. *science*, 313(5795):1929–1935, 2006.
- [26] Eric H Davidson. *The regulatory genome: gene regulatory networks in development and evolution*. Elsevier, 2010.
- [27] Ilya Shmulevich and John D Aitchison. Deterministic and stochastic models of genetic regulatory networks. *Methods in enzymology*, 467:335–356, 2009.

Supplementary information

Constructed exceptional network

It is possible to construct a network that has a fixed point with maximal control kernel $|\text{CK}| = n_c$ without having any isolated fixed points. Here we describe one such construction.

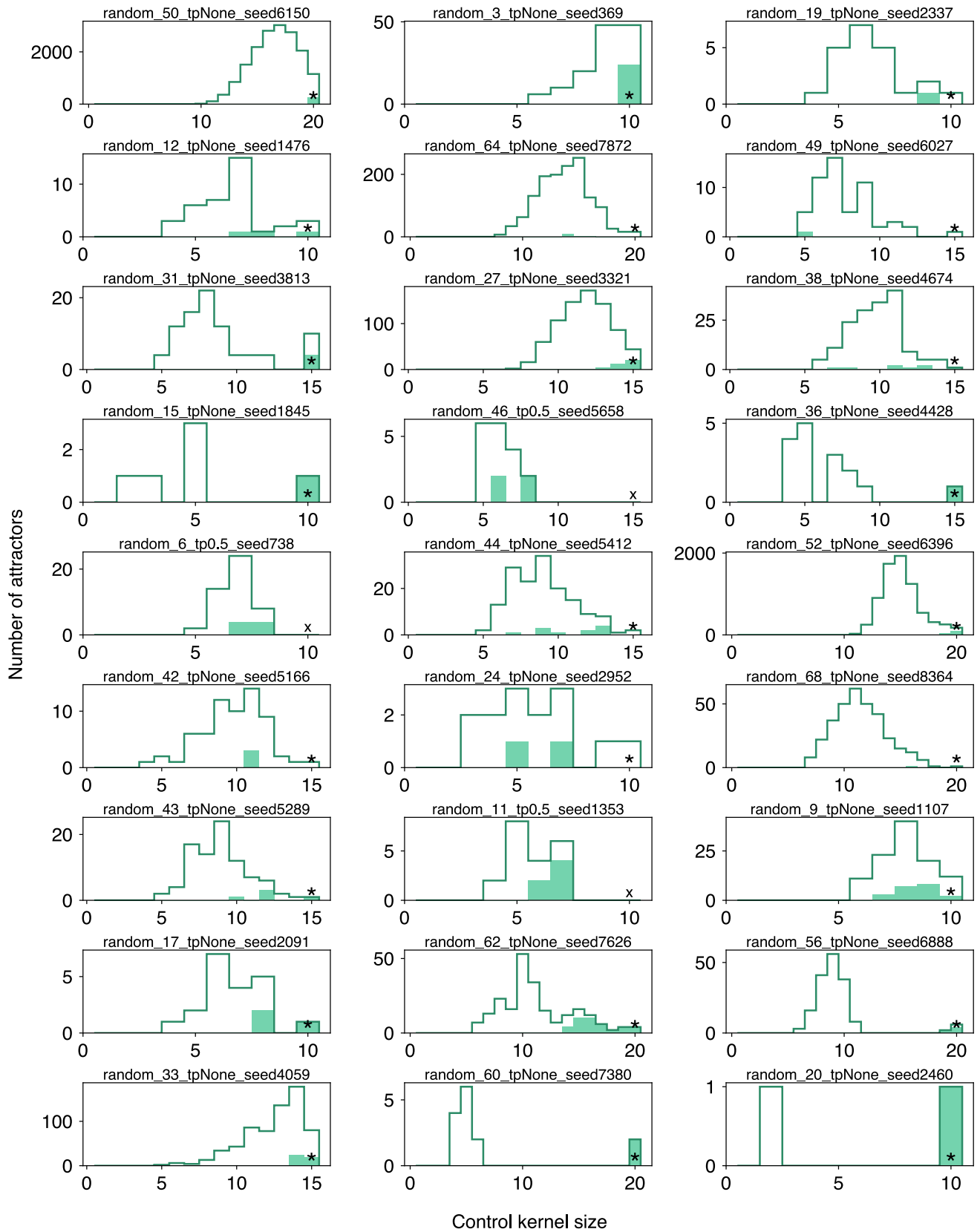
For the first node,

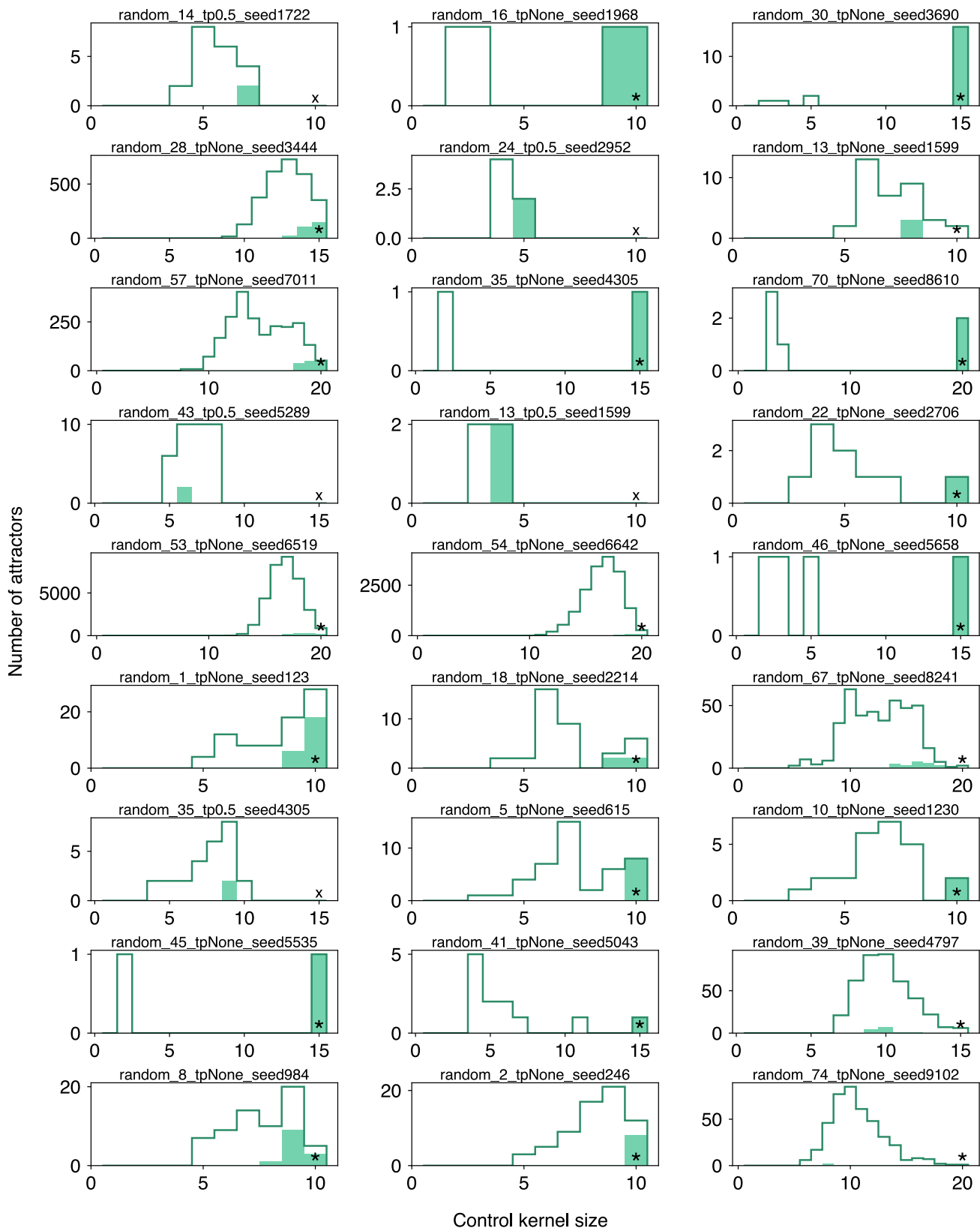
$$x'_1 = \begin{cases} 0 & \text{if } \sum_i x_i = 0 \text{ or } n \\ 1 & \text{otherwise} \end{cases} \quad (6)$$

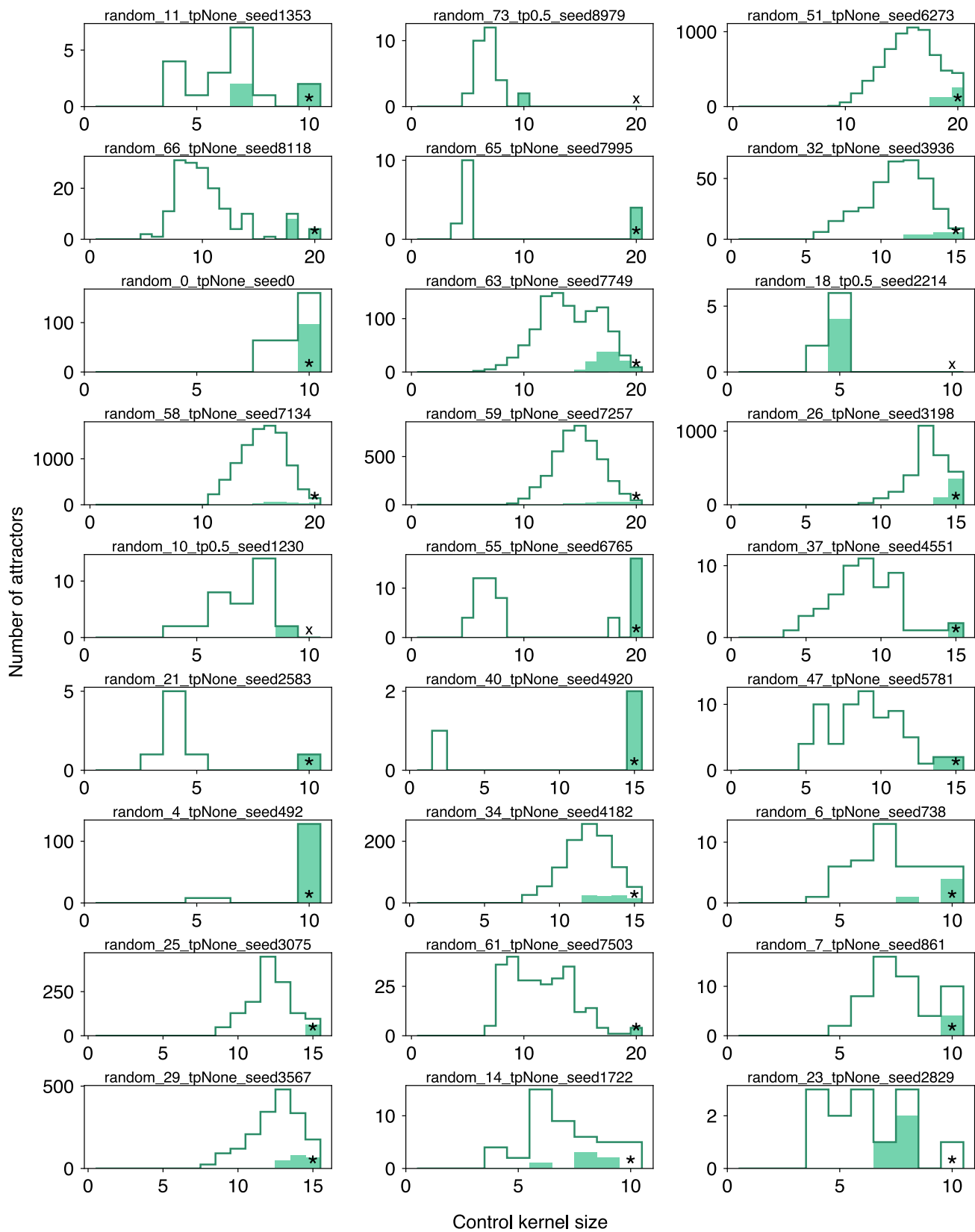
and for all other nodes j ,

$$x'_j = \begin{cases} 0 & \text{if } \sum_i x_i = 0 \text{ or } 1 \text{ or } n \\ 1 & \text{otherwise} \end{cases} \quad (7)$$

These dynamics produce two attractors: one in which all nodes are 0 and one in which all nodes are 0 except for the first. The control kernel for the second attractor is designed to have size n , but neither attractor has a basin size of 1 (specifically, the basin sizes are n and $2^n - n$).







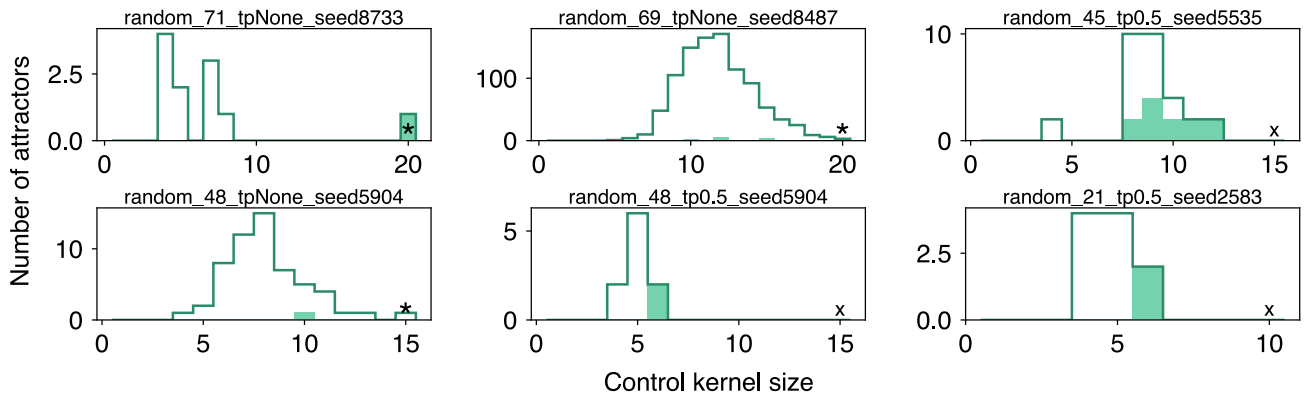


Figure S1: **Histograms of control kernel size for individual random networks with at least one isolated fixed point.** Control kernel sizes of all attractors are displayed with unfilled bars, and the subset corresponding to isolated fixed points are shown as shaded bars. A star is shown at n_c for those networks that have at least one control kernel of size n_c (73 networks), and an X is shown at n_c otherwise (14 networks).

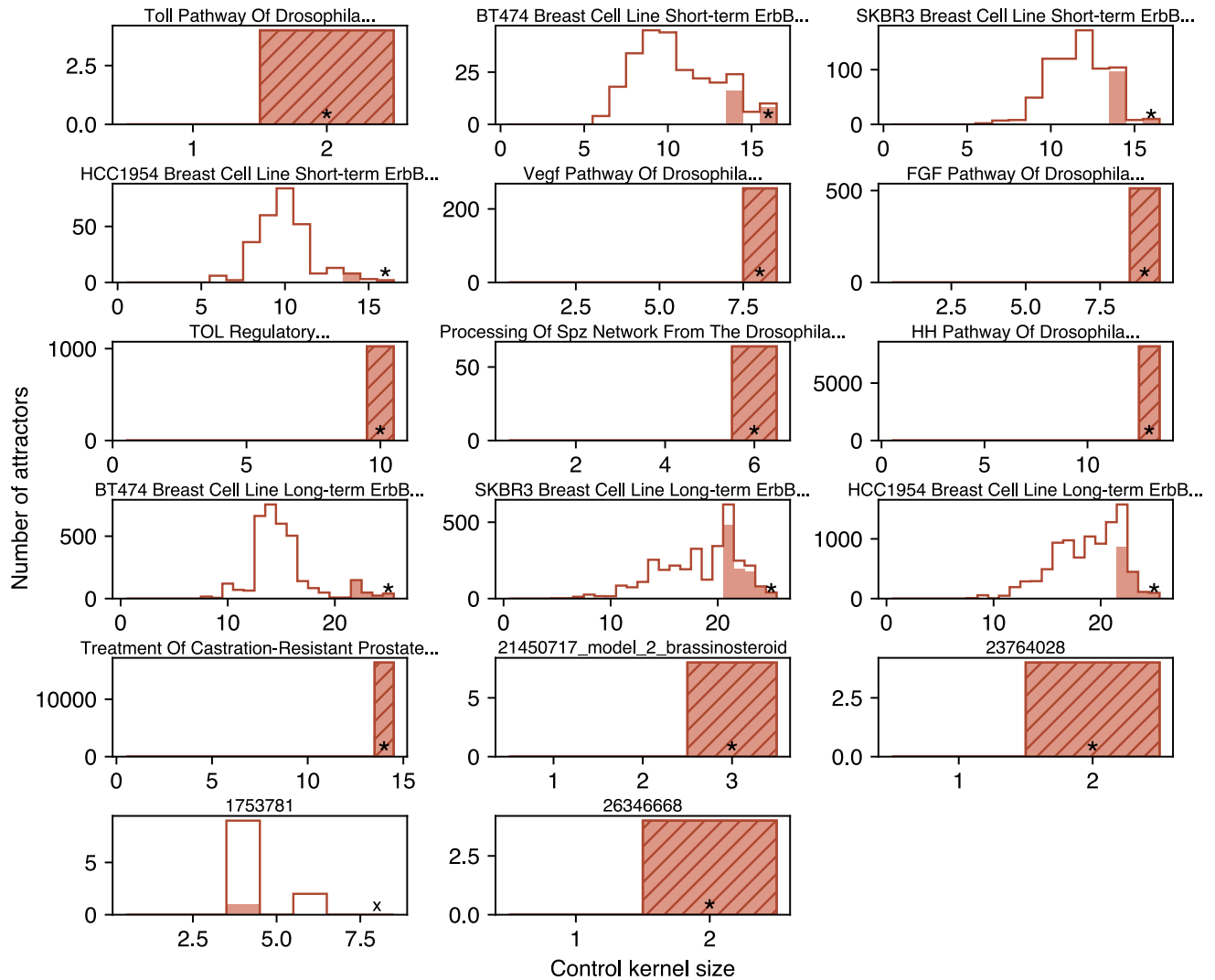


Figure S2: **Histograms of control kernel size for individual biological networks with at least one isolated fixed point.** Control kernel sizes of all attractors are displayed with unfilled bars, and the subset corresponding to isolated fixed points are shown as shaded bars. Networks without loops have histograms depicted with hatching, as in Fig. 2. A star is shown at n_c for those networks that have at least one control kernel of size n_c (16 networks), and an X is shown at n_c otherwise (1 network).

name	size	core nodes	mean CK size	attr.	isol. f.p.
	n	n_c	$\langle CK \rangle$	r	s
Arabidopsis Thaliana Cell Cycl...	14	14.0	0.0	1	0
B Cell Differentiation	22	20.0	5.9	61	0
BT474 Breast Cell Line Long-te...	25	25.0	14.0	3344	256
BT474 Breast Cell Line Short-t...	16	16.0	9.5	253	24
Body Segmentation In Drosophil...	17	12.0	3.4	10	0
Budding Yeast Cell Cycle	20	20.0	4.8	33	0
Budding Yeast Cell Cycle 2009	18	18.0	0.0	1	0
CD4+ T Cell Differentiation An...	18	18.0	8.6	324	0
Cardiac Development	15	15.0	2.8	6	0
Cell Cycle Transcription By Co...	9	9.0	1.0	2	0
Cortical Area Development	5	5.0	1.0	2	0
Death Receptor Signaling	28	25.0	4.7	97	0
FGF Pathway Of Drosophila Sign...	23	9.0	9.0	512	512
Fanconi Anemia And Checkpoint ...	15	15.0	0.0	1	0
Guard Cell Abscisic Acid Signa...	44	37.0	5.4	95	0
HCC1954 Breast Cell Line Long-...	25	25.0	17.8	9452	1504
HCC1954 Breast Cell Line Short...	16	16.0	9.0	274	10
HH Pathway Of Drosophila Signa...	24	13.0	13.0	8192	8192
Human Gonadal Sex Determinatio...	19	18.0	2.3	3	0
Iron Acquisition And Oxidative...	22	17.0	2.0	4	0
Lac Operon	13	13.0	3.2	9	0
Mammalian Cell Cycle	20	18.0	1.7	3	0
Mammalian Cell Cycle 2006	10	10.0	0.0	1	0
Metabolic Interactions In The ...	12	11.0	6.2	40	0
Neurotransmitter Signaling Pat...	16	14.0	2.0	4	0
Oxidative Stress Pathway	19	17.0	1.0	2	0
Predicting Variabilities In Ca...	15	15.0	2.8	6	0
Pro-inflammatory Tumor Microen...	26	26.0	2.5	6	0
Processing Of Spz Network From...	24	6.0	6.0	64	64
Regulation Of The L-arabinose ...	13	10.0	4.1	21	0
SKBR3 Breast Cell Line Long-te...	25	25.0	17.3	3185	960
SKBR3 Breast Cell Line Short-t...	16	16.0	10.7	702	104
Septation Initiation Network	31	29.0	9.4	2240	0
T Cell Differentiation	23	23.0	5.0	33	0
T-Cell Signaling 2006	40	10.0	3.1	10	0
T-LGL Survival Network 2011 Re...	18	17.0	2.3	3	0
TOL Regulatory Network	24	10.0	10.0	1024	1024
Toll Pathway Of Drosophila Sig...	11	2.0	2.0	4	4
Treatment Of Castration-Resist...	42	14.0	14.0	16384	16384
Trichostrongylus Retortaeformi...	26	25.0	3.2	12	0
Tumour Cell Invasion And Migra...	32	22.0	3.3	15	0
Vegf Pathway Of Drosophila Sig...	18	8.0	8.0	256	256
Wg Pathway Of Drosophila Signa...	26	23.0	14.0	16384	0
Yeast Apoptosis	73	30.0	13.3	11520	0

Table S1: Cell Collective networks [16].

PubMed ID	size	core nodes	mean CK size	attr.	isol. f.p.
	n	n_c	$\langle CK \rangle$	r	s
11082279	11	11	2.0	4	0
1753781	8	8	3.4	11	1
19524598	12	12	2.0	4	0
19622164_TGF_alpha	17	9	2.8	7	0
19622164_TGF_beta1	17	9	2.8	7	0
20169167	7	7	1.0	2	0
20221256_manual_mod	11	11	3.6	22	0
20659480	20	13	1.7	4	0
21450717_model_2_brassinostero...	10	3	3.0	8	8
21450717_model_4_2_BRX_integra...	20	17	3.0	14	0
21450717_model_5_1_BRX_integra...	20	17	2.0	4	0
21450717_model_5_2	20	17	2.0	4	0
21563979	13	13	3.2	9	0
21639591	25	25	2.0	4	0
21853041	11	11	2.7	8	0
22192526	9	8	3.0	7	0
23056457	17	16	3.8	12	0
23169817_high_dna_damage	16	16	0.0	1	0
23169817_low_dna_damage	16	16	0.0	1	0
23469179	10	9	3.1	8	0
23630177_metastatic_melanoma	10	9	2.0	4	0
23658556_model_1	14	14	3.8	10	0
23658556_model_2	16	16	3.2	9	0
23658556_model_3	15	15	3.8	9	0
23658556_model_4	17	17	3.0	10	0
23658556_model_5	15	15	3.1	8	0
23658556_model_6	15	15	3.1	8	0
23658556_model_7	17	17	4.5	14	0
23658556_model_8	16	16	4.1	12	0
23658556_model_9	17	17	3.2	9	0
23764028	5	2	2.0	4	4
24376455	10	9	2.0	4	0
24564942_threshold	8	8	2.6	5	0
25163068	30	27	7.3	241	0
25967891	13	12	4.1	10	0
26244885	30	29	8.4	1104	0
26346668	30	2	2.0	4	4
27613445	25	23	3.6	22	0
28187161	30	27	6.8	220	0
28209158	9	9	1.7	3	0
28426669_ARF10_greater_ARF5	16	15	3.3	14	0
28426669_ARF10_smaller_ARF5	16	15	3.3	14	0
28455685	15	15	2.0	4	0
29186334	29	16	5.2	25	0
29596489	23	18	2.2	5	0
30024932	21	16	2.3	6	0
30104572	5	5	2.0	3	0
30148917	18	14	4.0	16	0
30323768	21	16	3.8	18	0
30530226	23	19	2.0	5	0
30546316	30	21	10.6	1056	0
31949240	24	21	5.4	45	0
32054948	27	24	2.2	6	0

Table S2: Additional biological networks from [14].